NJC

Dynamic Article Links

Cite this: *New J. Chem.*, 2012, **36**, 603–612

www.rsc.org/njc

PAPER

Engineering *N*-(2-pyridyl)aminoethyl alcohols as potential precursors of thermolabile protecting groups†

Marcin K. Chmielewski,*[a] Ewa Tykarska,[b] Wojciech T. Markiewicz[a] and Wojciech Rypniewski[a]

Received (in Montpellier, France) 5th July 2011, Accepted 10th November 2011
DOI: 10.1039/c1nj20584f

Crystal and NMR analyses of four precursors of *N*-(2-pyridyl) thermolabile protecting group (TPG) were carried out. Two torsion angles have been identified as indicators that predict the molecules' thermolabile properties. Conformation that minimizes the N1···C8 distance is crucial for thermocyclisation. Nucleophilicity of the pyridyl ring is the driving force for the reaction but it is insufficient for thermocyclisation which is dominated by the molecules' ability to adopt a favourable conformation. The pK_a value was recorded for all analyzed *N*-(2-pyridyl)aminoethyl alcohols. However, its effect is small in the determination of thermolability. Based on the analysis that we carried out, *N*-benzyl *N*-(2-pyridyl)aminoethyl was selected as a potential precursor of thermolabile carbonate of TPG.

Introduction

Thermolabile protection is a new approach in modern organic chemistry, in which a thermolabile protecting group (TPG), stable at ambient temperature, is used to temporarily block the reactive site in a multifunctional compound. Upon increasing the temperature, the TPG blocking group is removed, *e.g.* by intramolecular cyclization, and the free state of the protected function is restored. One of the most important applications of TPG is the chemical synthesis of DNA.[1] In this approach, TPG is used to protect phosphate/thiophosphate, hydroxyl or amine functional groups.[2] Several different classes of molecules including 2-(*N*-formyl-*N*-methylamino)ethyl,[3] 4-oxopentyl,[4] 3-(*N*-*tert*-butylcarboxamido)-1-propyl,[5] 3-(2-pyridyl)-1-propyl,[6] and 2-benzamidoethyl groups[7] have been successfully employed as phosphate/thiophosphate thermolabile protecting groups. However, they have often been found to be more labile than other phosphate protecting groups. Therefore, the "click-clack" approach has been used to increase the stability of TPG as protectants of the phosphate center.[8] The thermolytic protection of the hydroxyl function, on the other hand, is most successfully done through the use of carbonates. The thermodeprotection of the carbonate as the TPG proceeds through the intramolecular attack of the nucleophilic center on the electrophilic α carbon atom. In such cases, deprotection involves the release of carbon dioxide in the cyclodecarbonation process. The advantage of thermolabile groups over the previously known photolabile carbonates[9] is that in the case of TPG no free radicals are formed during the deprotecting process. Based on its chemical properties, the *N*-(2-pyridyl) moiety has been identified as a very effective nucleophilic center, and carbonates of *N*-(2-pyridyl)aminoethanols have been proposed as possible thermolabile protecting groups.[10] A new protecting system for a hydroxyl group, based on thermal cyclodecarbonation, has been described recently, in which the *N*-(2-pyridyl)aminoethanol [*N*-(2-PAE)] is converted to thermolytic carbonates.[11] *N*-(2-PAE) alcohols, first synthesized in 1949 by Weiner and Kaye,[12] are among the promising candidates for efficient precursors of TPG in oligonucleotide synthesis.

The main objective in engineering effective protective TPGs is their stability at ambient temperatures and lability under rising temperature. This can be achieved by regulating the nucleophilic character of the pyridyl ring. There are three main ways by which the nucleophilic properties of pyridine nitrogen can be affected: (1) by hydrogen bonding involving the pyridine nitrogen, (2) incorporating electron-donating and electron-withdrawing substituents, (3) steric and structural influence. However, it is not easy to draw clear conclusions regarding the thermolability of carbonates on the basis of the structure of the precursor *N*-(2-PAE) alcohol alone. By looking at a wide range of derivatives, one can try to establish the correlation between certain characteristics of their structures (resulting from different types of substitution) and the dominant effect on the nucleophilic center. In our studies, we have focused on exploring different

[a] *Institute of Bioorganic Chemistry, Polish Academy of Science, Noskowskiego 12-14, 61-704, Poznań, Poland. E-mail: maro@ibch.poznan.pl; Fax: +48 618520532; Tel: +48 618528503*
[b] *Department of Chemical Technology of Drugs, Poznan University of Medical Sciences, Grunwaldzka 6, 60-780, Poznań, Poland*

† Electronic supplementary information (ESI) available: Materials and methods; synthesis and characterization of compounds **1–5**, ^{1}H NMR and X-ray tables, potentiometric measurements, ^{1}H, ^{13}C and two dimensional NMR, MS spectra and analysis of thermostability of **4**. CCDC 827067 (**1**), 827068 (**2**), 827069 (**3**), 827070 (**4**), and 827071 (**5**). See DOI: 10.1039/c1nj20584f

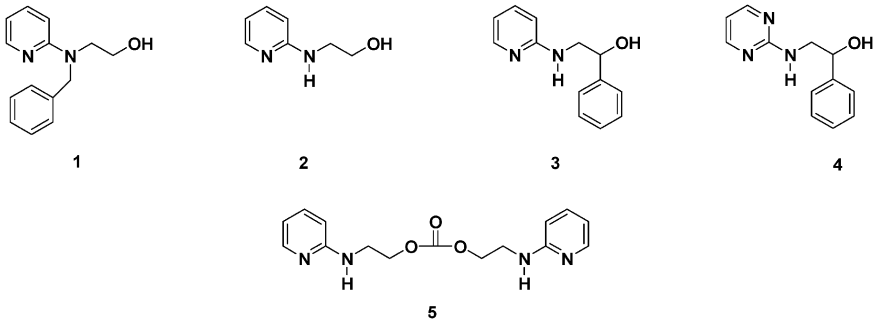

Scheme 1 Structures of 2-(2-PES) alcohols, symmetric carbonate.

ways of chemical modification of *N*-(2-PAE). Here we report the synthesis, the physicochemical properties and crystallographic analysis of four *N*-(2-PAE) alcohols as precursors of TPG (Scheme 1), and one structure of a symmetric carbonate derived from one of the *N*-(2-PAE) alcohols as a model of a carbonate protecting group.

Although thermolability is observed in the solution, it is more difficult to precisely characterize the structures of molecules in the liquid state than in the crystal state. It is worth noting that the crystal structure represents some energy minimum. Fortunately, many structural characteristics, especially the inter- and intramolecular interactions observed in the crystal, also occur at the equilibrium of molecular conformations in solution. The aim of this study is to find the relationship between the structure of TPG and its thermolability. Here we have analyzed the crystal structures and physicochemical properties of the four *N*-(2-PAE) derivatives and focused on the structural characteristics relevant to the thermolytic protection. In particular, we demonstrate the important role of hydrogen bonds in controlling the properties of the nucleophilic center in solution and in the crystalline state.

Results/discussion

The important feature of thermolytic carbonates acting as an efficient hydroxyl protectant is the intramolecular thermolytic cyclodecarbonation which follows from the interaction between the pyridyl nitrogen and the electrophilic carbon atom (C8). As a result of intramolecular thermocyclization of the TPG a bicyclic by-product was formed concurrently with the release of carbon dioxide (Scheme 2). Except for the pyridine ring, the bicyclic product also contains a five-membered ring. Formation of this five-membered ring is important in the analysis of deprotection and further discussion is focused on it. In order to find the optimal TPG, we have undertaken a systematic analysis of the structures of aminoalcohol precursors of TPG to determine the modification of features that influence the kinetics of cyclization. By modifying TPG one can change the properties of the nucleophilic and electrophilic centers and

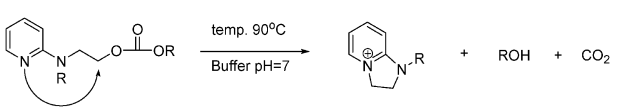

Scheme 2 Thermal cyclization. The scheme of TPG unblocking.

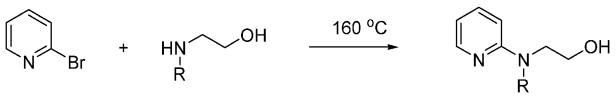

Scheme 3 Synthesis of precursor of TPG 2-pyridyl aminoethanol derivatives.

parameters of the protecting group, such as the speed of unblocking.

After that, synthesis and crystallization were carried out and followed by an investigation of the physicochemical properties of several different aminoalcohols and a model symmetric carbonate. The preparation of *N*-(2-PAE) alcohols was carried out according to the general scheme by reacting the corresponding N-substituted aminoalcohol with 2-bromopyridine (Scheme 3).

Symmetric carbonates were prepared by condensation of 1,1′-carbonyldiimidazole with **2**.

Analysis of thermostability of TPG

Previously, compounds **2** and **3** had been transformed into thermolabile carbonates and investigations were carried out to determine the kinetics of their unblocking.[10] Complete deprotection of TPG formed from precursor **2** was achieved in 1.5 hours. Acceleration of this reaction of deprotection took place when the precursor **3** was used for corresponding TPG (30 min).

Based on these results, one can conclude that the presence of an aromatic ring attached to α carbon (C8) significantly accelerates the unblocking reaction. The disadvantage of this approach is that a substitution at the α carbon (C8) results in a chiral center. Diastereoisomers are obtained when blocking the hydroxyl group of a compound which has a specific configuration (*e.g.* nucleosides).

Three TPG precursors (**2–4**) presented here have a hydrogen atom at the *exo*-amine N2 atom. The previous study[10,11] showed that substituting this amine hydrogen with an alkyl group considerably affects the speed of the unblocking reaction. The probable reason is that strong electron-donating substituent enhances the electron resonance between the pyridyl ring and the *exo*-amine N2. As a consequence of the resonance the nucleophilicity of N1 (its electron density) of the pyridine ring increases, which favors thermolability. Following this trail we proposed compound **1** in which the benzyl substituent is expected to increase the nucleophilicity of pyridine nitrogen. Additionally, by introducing a benzyl group at *exo*-amine N2 (compare **3** and **4**) one can avoid the formation of a chiral compound.

Table 1 The pK_a values. Apparent pK_a were measured by titration of 1.25×10^{-2} M solutions of hydrochloride acid in methanol–water (1 : 1) or acetonitrile–water (3 : 1) with 3.04×10^{-2} M NaOH at 25 °C. The deprotection time for the carbonates obtained from a corresponding precursor was designated in the solution of acetonitrile/buffer pH = 7 at 90 °C (1 : 1) and calculated on the basis of RP HPLC analysis

	1	2	3	4	5
MeOH–H_2O	5.44 ± 0.02	6.24 ± 0.02	6.07 ± 0.02	3.58 ± 0.11	4.97 ± 0.04 6.42 ± 0.03
CH_3CN–H_2O	5.39 ± 0.02	6.28 ± 0.02	6.08 ± 0.02	3.26 ± 0.06	
Total deprotection time of carbonates	8 minutes	120 minutes	60 minutes	50 minutes	

As it turned out, however, the change of the heterocyclic ring into a less nucleophilic 1,3-pyrimidine ring (precursor **4**) does not affect the speed of deprotection of TPG's reaction.[13] In this context, electron density appears as a less significant factor influencing the speed of thermocyclization, and the decisive factor in this process is probably of conformational origin.

Physical properties, pK_a values

The pK_a values were determined for all aminoethanols **1–4** and for the model symmetric carbonate **5**. Measurements were carried out in two different solvents. These data indicate that the most basic is compound **2**. The presence of an additional aromatic ring in **1**, **3**, **4** lowers their basicity. The effect is stronger if the rings are located close to the nucleophilic center. A significant drop in the basicity is observed as a result of change of the pyridine to pyrimidine ring. Lowering the basicity facilitates the construction of TPG. However, excessively low basicity can weaken the nucleophilic character of the pyridyl center (Table 1).

A comparison of basicity/nucleophilicity of the TPG precursors with the reactivity of corresponding thermolytic carbonates does not give a simple relationship. Compounds **2** and **3**, leading to TPGs with very different times of deprotection, have a similar pK_a value. Conversely, pK_a of compounds **3** and **4** with similar reaction times differ by nearly **3**. Therefore, the nucleophilic properties of a molecule and its ability to interact with a proton seem to be important in thermocyclization but are not the only factors determining the stability of corresponding TPGs.

Crystallographic results

The structures of four precursors of TPG and one model TPG were determined by X-ray crystallography (Fig. 1). The analysis has shown that the N1···C8 distance is crucial for the speed of thermocyclisation and it depends on two torsion angles: N1–C2–N2–C7 and C2–N2–C7–C8, which in the flat five-member ring (part of the bicyclic product formed during intramolecular thermocyclisation) have a value 0°. In the presented structures the first torsion angle always takes values

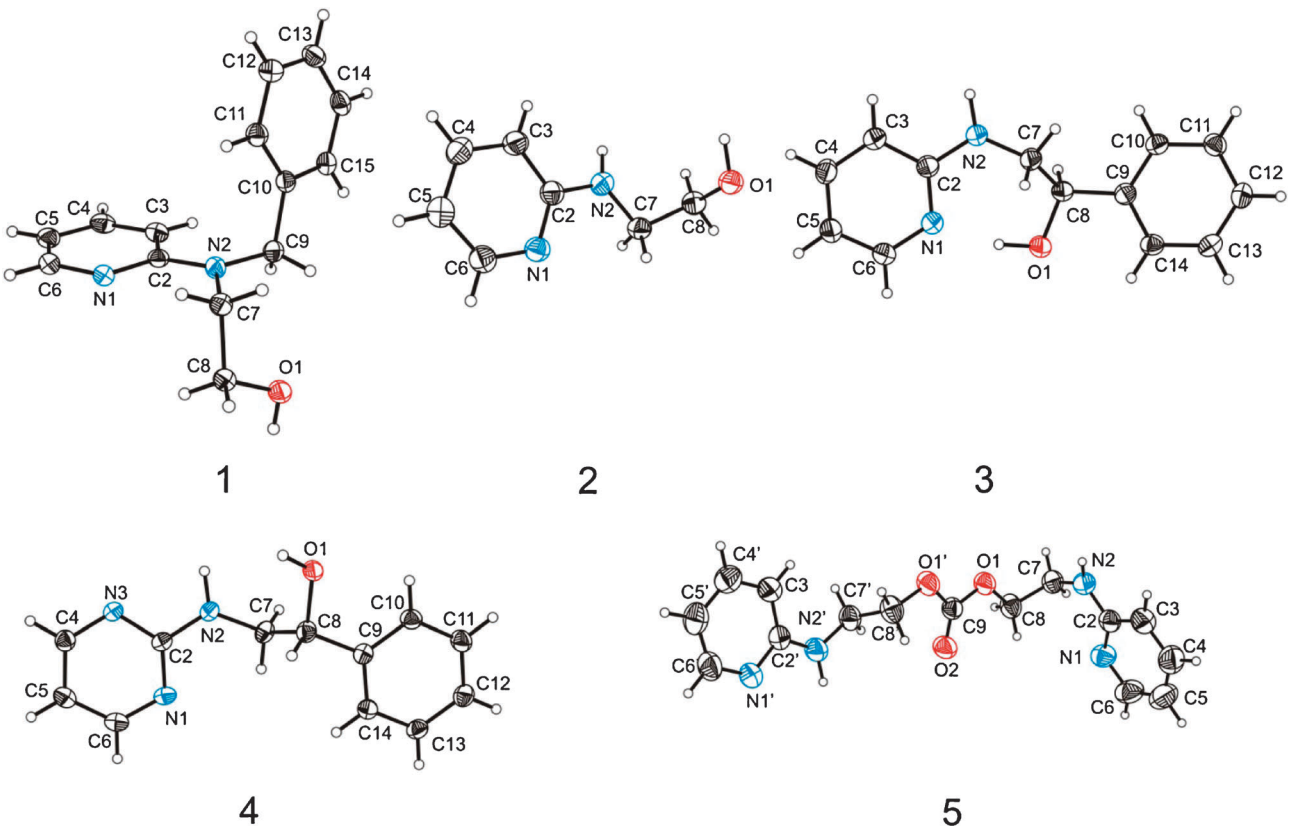

Fig. 1 The molecular structures of **1** to **5**, showing the atom labeling scheme. Displacement ellipsoids are drawn at the 50% probability level and H atoms are shown as spheres of arbitrary radii. Only one major orientation of disordered oxygen in **4** is presented.

Table 2 X-Ray experimental details of **1** to **5**

	1	**2**	**3**	**4**	**5**
Formula	$C_{14}H_{16}N_2O$	$C_7H_{10}N_2O$	$C_{13}H_{14}N_2O$	$C_{12}H_{13}N_3O$	$C_{15}H_{18}N_4O_3$
fw	228.29	138.17	214.26	215.25	302.33
Crystal system	Monoclinic	Orthorhombic	Orthorhombic	Monoclinic	Monoclinic
Space group	$P2_1/n$	$Pca2_1$	$P2_12_12_1$	$P2_1/c$	$C2/c$
a/Å	10.756(2)	8.841(2)	6.048(1)	5.605(1)	32.33(7)
b/Å	5.926(1)	9.053(2)	7.315(2)	20.972(4)	5.791(1)
c/Å	18.840(4)	8.630(2)	24.334(5)	9.500(2)	16.392(3)
β/°	99.58(3)			108.1(3)	104.42(3)
V/Å^3	1184.1(4)	690.7(2)	1076.6(4)	1061.4(4)	2973.7(10)
Wavelength/ Å	0.81620	0.8125	0.81620	0.81620	0.80800
Z	4	4	4	4	8
Resolution range/Å	20.0–0.76[a] (0.77–0.76)	10–0.75 (0.76–0.75)	20.0–0.75 (0.76–0.75)	20.0–0.75 (0.76–0.75)	10.0–0.75 (0.76–0.75)
D_c/gcm^{-3}	1.281	1.329	1.322	1.347	1.351
μ/cm^{-1}	0.082	0.092	0.085	0.089	0.097
R_{merge}[b]	0.032 (0.039)	0.050 (0.135)	0.037 (0.095)	0.028 (0.057)	0.045 (0.086)
R_1 (obs. data)	0.0449	0.0435	0.0442	0.0471	0.0451
wR_2 (obs. data)	0.1207	0.1213	0.1229	0.1321	0.1283
Independ refs	2806	906	1572	2574	3622
Refs $I > 2\sigma(I)$	2732	885	1527	2522	3471

[a] Values in parentheses are for the last resolution shell. [b] $R_{merge} = \Sigma_{hkl}\,\Sigma_i|I_i\,(hkl) - \langle I(hkl)\rangle|/\Sigma_{hkl}\,\Sigma_i\,I_i\,(hkl)$, where $I_i\,(hkl)$ and $\langle I(hkl)\rangle$ are the observed individual and mean intensities of a reflection with the indices hkl, respectively, Σ_i is the sum over i measurements of a reflection with the indices hkl, and Σ_{hkl} is the sum over all reflections.

close to 0° (*syn* conformation of TPG precursors) or 180° (*anti* conformation) because in all investigated compounds, the *exo*-amine N2 atom has planar sp^2 hybridization and all atoms bonded to the *exo*-amine N2 atom are coplanar with the heterocyclic ring, *i.e.* the dihedral angle between the heterocyclic ring and C2–N2–C7 planes is close to 0° (Table 2).

Thus, there is a significant involvement of the N2-amine lone pair of electrons with the π-system of the pyridine/pyrimidine ring which is accompanied by shortening of the N2–C2 bond from 1.419 Å, expected for $C_{aromatic}$–N(sp^3), to the observed average of 1.37 Å which is close to a typical value for $C_{aromatic}$–N(sp^2) bond length of 1.353 Å.[14] This conjugation between the electron lone pair of the amine nitrogen and the heterocyclic π electrons favors *syn* or *anti* conformers of TPG precursors. Analysis of torsion angles N1–C2–N2–C7 in compounds **4** and **5** has shown that shorter distance N1···C8 is observed when this torsion angle is close to 0°. In compound **4** the distances are 3.896(2) and 4.626(1) Å for N1–C2–N2–C7 (8.3°) and N3–C2–N2–C7 (−172.1°), respectively, and the distance N1···C8 in **5** is 3.198(2) Å in *syn* and 4.376(1) Å in *anti* conformers. In all investigated compounds the N1···C8 distance also depends on the C2–N2–C7–C8 angle and it decreases with the decreasing absolute value of this torsion angle (Table 3).

The smallest N1···C8 distance, close to the sum of the van der Waals radii, has been found in *syn* conformers of **1**, **3** and **5** with the absolute value of the second torsion angle less than 90° (Table 3).

Thus, the shortest distance N1···C8 requires (i) the N1–C2–N2–C7 torsion angle close to 0° and (ii) a possibly smallest absolute value of the C2–N2–C7–C8 torsion angle. Therefore, we postulate that restricting rotational freedom around C2–N2 and N2–C7 bonds in order to maintain (i) and (ii) favors the N1···C8 interaction. In all the investigated compounds, free rotation of C2–N2 is restricted by its partially double bond character. Additionally, steric hindrance is observed in **1**, compared to **2**, due to a large substituent at the *exo*-amine N2 atom which traps the C8 between N1 and C9. In **1** the N1···C8, a distance of 3.399(2) Å, and C8···C9, a distance of 3.298(2) Å, are close to the sum of the atoms van der Waals radii, and restrict the rotation around N2–C7. Thus, the C2–N2–C7–C8 torsion angle of 84.5(1)° (Table 3) is almost optimal for thermocyclization. In **2**, although the TPG precursor is in *syn* conformation, the free N2–C7

Table 3 Selected bond distances (Å) torsion angles (°) and dihedral angles between planes for **1–5**. Numbers in parentheses represent standard deviations

	1	**2**	**3**	**4**	**5**
Bond lengths/Å					
N2–C2/N2′–C2′	1.370(1)	1.366(2)	1.375(2)	1.352(1)	1.366(1)/1.361(1)
Distances/Å					
N1···C8/N1′···C8′	3.399(2)	4.272(3)	3.231(3)	3.896(2)	3.198(2)/4.376(1)
N3···C8				4.626(1)	
Torsion angles/°					
N1–C2–N2–C7/N1′–C2′–N2′–C7′	7.9(1)	2.2(3)	17.9(3)	8.3(1)	0.4(1)/−178.01(9)
N3–C2–N2–C7				−172.08(8)	
C2–N2–C7–C8/C2′–N2′–C7′–C8′	84.5(1)	−162.7(2)	−82.8(3)	−118.8(1)	75.1(1)/83.9(1)
Dihedral angles/°					
N1–C2–C3/N3–C4–C5–C6 and C2–N2–C7	3.37(8)	1.9(3)	16.7(3)	8.5(1)	1.8(2)
N1′–C2′–C3′–C4′–C5′–C6′ and C2′–N2′–C7′					2.5(2)

rotation makes this compound suboptimal for N1···C8 interaction. Compounds **3** and **4** were designed to test the effect of electron withdrawing by the phenyl group on atom C8, *i.e.* it would deplete electrons at the carbon atom and promote its interaction with N1. It seems to be the case in **3**, where the C8···N1 distance is closest. Compound **2** which lacks the phenyl group has the C8···N1 distance 1 Å longer. However, it is interesting to note that compound **4**, in which the N1···C8 distance is much longer than the sum of the van der Waals radii (3.826(2) Å) and the nitrogen atom is less basic than in pyridine, which implies a slower reaction, has in fact the reaction speed comparable to compound **3**.

The presence of the second nitrogen atom in the pyrimidine ring guarantees a *syn* conformation at N1(or N3)–C2–N2–C7 with respect to one of the *endo*-N atoms, doubling the availability of optimal conformers in comparison with pyridine. This favours the speed of thermocyclisation. One drawback of **3** and **4** is their chirality and subsequent racemic nature of derived reaction products. Curiously, **3** is crystallized in non-centrosymmetric space group $P2_12_12_1$ and the crystal contains one enantiomer (it was not possible to determine which one). Compound **5** is a carbonate derivative of **2**. In our studies, **5** was a model of a carbonate thermolabile protecting group. Crystallographic analysis revealed that despite its chemical symmetry, each half of the compound has a different conformation. Nevertheless, one part has a similar structure to the corresponding alcohol despite the transformation of the hydroxyl group to carbonate. It is possible that other alcohols may also retain their conformation upon their conversion to thermolabile carbonates. Unfortunately, they were not sufficiently stable for crystallographic studies.

Based on the structural analysis of precursor and kinetics of thermocyclization in target carbonates, we postulate that the N1···C8 distance has a key significance for the stability of a thermolabile protecting group and the two torsion angles which take values close to 0°, once the five-membered ring is formed, are crucial for the intramolecular thermocyclization based on the interaction between the two atoms. One can reasonably assume that the observed structure corresponds to an energy minimum and the conformation observed in the crystal will also be present in solution.

Hydrogen bonds in crystal structures

The *syn* and *anti* conformers make different kinds of hydrogen networks. In *syn* the O···N hydrogen bonds are present while in *anti* N···N dimers form the main hydrogen pattern. Wherever possible, O1 in *syn* is both a donor and an acceptor, and NH···OH···N bonds are formed.

In all the investigated compounds the *exo*-amine and hydroxyl groups are involved in intermolecular hydrogen bonding except **3**, where an intra-hydrogen bond is present (Fig. 2 (1–5) and Table 4). Intramolecular H-bonds in **3** may restrict rotation about N2–C7 and contribute to stabilization of the close contact N1···C8. However, this effect will be absent after transformation to a corresponding carbonate and its structure is likely to be different. Compounds **1**, **2** and **4** do not form intramolecular H-bonds, therefore their structure is not affected in this way by the transformation of a hydroxyl group to carbonate.

Table 4 Hydrogen bonds geometry (Å, °) for **1–5**

Compound	D–H···A	D–H	H···A	D···A	D–H···A
1	O1–H1···N1[1]	0.89	1.97	2.8236(12)	161
2	N2–H2···O1[2]	1.00	1.95	2.906(2)	160
	O1–H1···N1[3]	1.00	1.82	2.798(2)	167
3	N2–H2···O1[4]	1.01	2.00	2.973(2)	161
	O1–H1···N1	1.03	1.74	2.754(2)	166
4	O1–H1···N1[5]	0.93	1.99	2.912(9)	168
	O1'–H1'···N1[5]	0.88	2.10	2.911(11)	153
	N2–H2···N3[6]	0.97	2.04	3.0070(16)	170
5	N2'–H2'···N1[7]	0.95	2.19	3.1188(14)	168
	N2–H2···O2[8]	0.91	2.09	2.9819(12)	166

Symmetry codes: (1) $-x + 1/2, y - 1/2, -z + 1/2$; (2) $-x + 1/2, y, z - 1/2$; (3) $x - 1/2, -y, z$; (4) $x - 1, y, z$; (5) $x - 1, y, z$; (6) $-x - 1, -y + 1, -z + 1$; (7) $-x + 1/2, -y + 3/2, -z + 1$; (8) $x, y - 1, z$.

In alcohols **1–4**, bonds O–H···N are dominant in the structural arrangement of molecules. In these compounds, the number of H-bond donors equals the number of acceptors and all are involved in bonding. The dominant H-bond in the resulting compound **5** is O···H–N. Because the molecule has two donors and three acceptors, the symmetry is broken and one weak acceptor (aromatic *N* atom) remains without an H-bonding partner. This entails a structural asymmetry in the chemically symmetric compound: the first half involved in the H-bonding interaction with a carbonyl oxygen atom that takes up *syn* conformation (similarly to its parent compound **2**), whereas the second half remains *anti*. (Fig. 2).

Analysis of hydrogen bonds in this study has provided some information about the structures of *N*-(2-PAE) alcohols and gives insight into new possibilities in the studies of thermolabile protecting groups.

NMR analysis

First we employed ^{1}H NMR, ^{13}C NMR spectroscopy to obtain information about the position and correlation of hydrogen atoms in the structures. The NMR spectra were recorded in deuterated DMSO and high quality of coupling was observed. The amine proton (sp^2) in **2**, **3**, **4**, and **5** that is bonded with the pyridyl ring has aromatic character. This is evident from the values of their chemical shift, which range from 6.4 to 6.9 ppm. In this study, we also analyzed the two dimensional spectra for correlating the location of all atoms (see ESI†).

We have employed ^{1}H–^{1}H two dimensional (2D) NMR spectroscopy to obtain higher resolution information about the conformation of *N*-(2-PAE). The Nuclear Overhauser Effect spectroscopy (NOESY) was used to determine the position of hydrogen atoms and revealed the conformation of the molecule in solution. All observations of the NMR study were compared with the molecular structure obtained by crystallography.

Fig. 3 shows the expanded region of the ^{1}H–^{1}H NOESY spectrum of compound **1** in deuterated DMSO. We observed a strong NOEs cross peak between hydrogen at the C-3 atom from the pyridyl ring and hydrogen atoms at C7, C8 and C9 from the benzyl group. This suggested a close contact of these hydrogen atoms and a coexistence of structures with the *syn* and *anti* conformers of the torsion angle N1–C2–N2–C7. One of

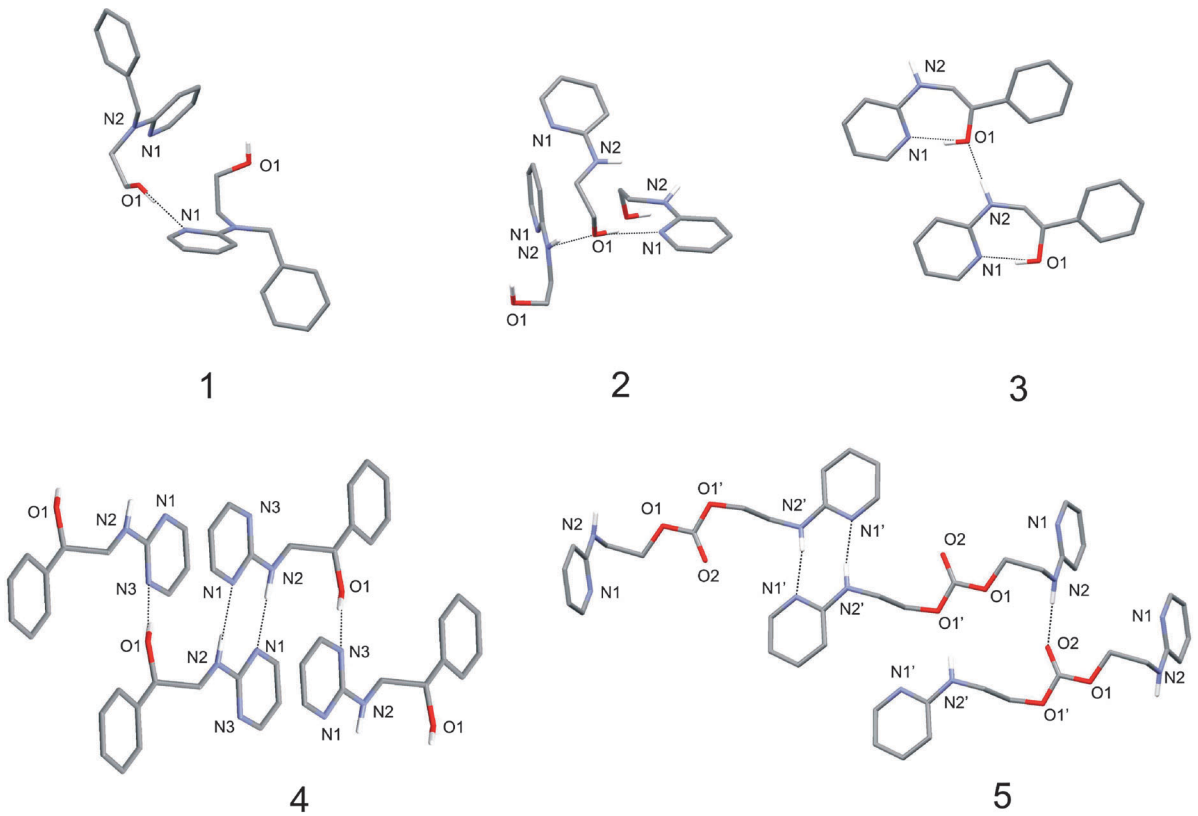

Fig. 2 Hydrogen bond patterns in **1** to **5**.

them is similar to a crystallographic structure. Additionally, we also observed a strong cross peak between one part of the phenyl group and the same C7, C8 and C9 hydrogen atoms. This observation suggested a twist of the benzyl group towards the aliphatic chain and a low value of the second torsion angle C2–N2–C7–C8 (Table 5).

In compounds **2–4**, the *exo*-amine proton plays a key role in shaping the structure. This finding is supported by the results of the D_2O exchange experiments (replacing all labile protons with deuterium) which showed a disappearance of the NOEs peaks for interactions with the *exo*-amine proton. Fig. 4 demonstrates the expanded region of the NOESY spectrum for experiments with and without D_2O. This comparison showed the elimination of cross peak from interaction of a labile amine proton. In the case of compound **2**, interaction only between hydrogen atoms at C3 and C8 was observed suggesting that the molecule has a torsion angle N1–C2–N2–C7 tending to the *anti* conformation and the C2–N2–C7–C8 torsion angle adopting a conformation with an intermediate value. In such a situation, the diagnostic distance N1···C8 for thermocyclization has a large value which will result in slowing down this reaction. In the spectrum of **3**, we observe a very weak NOE peak associated with a hydrogen at C3. This observation suggested that the torsion angle N1–C2–N2–C7 is close to *syn* conformation. In compound **4**, the diagnostic C3 hydrogen was absent. The analysis of interaction of the *exo*-amine proton provides information about torsion angle C2–N2–C7–C8. In compounds **2** and **5**, the *exo*-amine protons give a strong NOEs cross-peak with the C8 hydrogen and a slightly weaker peak with the C7 hydrogen which corresponds to intermediate values of this angle. But in **3** and **4**, interaction with hydrogen at C8 was stronger, which is typical for high absolute values of the torsion angles C2–N2–C7–C8.

Concluding remarks

Thermolabile protecting groups (TPGs) can be a very useful tool in the chemical synthesis of biologically active molecules. In order to find optimal TPG in terms of structure and properties, we carried out a structural analysis of aminoalcohols, the precursors of these groups. Observations were made, which could lead to a range of new thermolabile protecting groups. In the thermocyclization reaction, the substrates are carbonates, but they are difficult to study, because they are unstable. Instead, the precursor alcohols have been examined.

X-Ray analysis of the precursors has allowed for an identification of the basic parameters in thermocyclization reactions. In our opinion, the distance between the *endo*-N1 nitrogen atom and the C8 atom is an important feature in thermocyclization and the subsequent removal of the corresponding thermolabile protecting groups. Shortening the distance is expected to facilitate the reaction. Two torsion angles are important in this respect: N1–C2–N2–C7 and C2–N2–C7–C8. To shorten the N1···C8 distance the conformation of both torsion angles as close as possible to 0 angle. In the crystal structure, the first angle is *syn* in all the examined structures except one conformation in **5**, where *anti* occurs in conjunction with an intermolecular H-bond. The optimal conformation of the second angle (absolute value less than 90°) can be stabilized by two types of interactions: (i) steric, like in **1**, by means of an

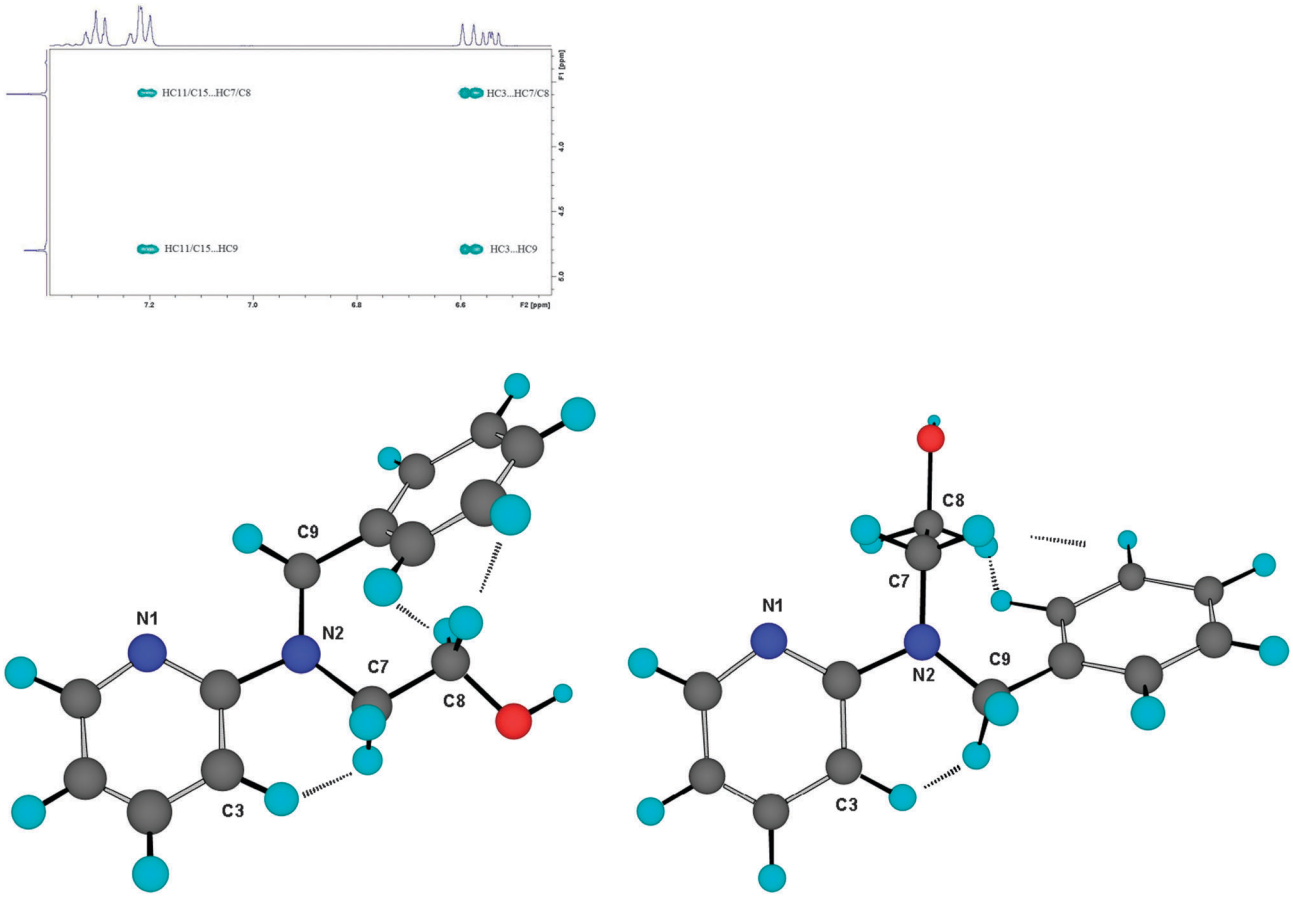

Fig. 3 At the top there is an expanded NOESY contour plot for **1**. At the bottom there are two structures that are dominant in solution: on the left—*anti* and on the right—the *syn* conformation.

Table 5 Approximate conformation of diagnostic torsion angles estimated on ^{1}H–^{1}H NOESY NMR spectra

	Compound			
Torsion angles	**1**	**2**	**3**	**4**
N1–C2–N2–C7	*syn* and *anti*	*anti*	*syn*	X
C2–N2–C7–C8	Close to zero	~90°	Close to zero	~90°

aromatic substitution at N2, (ii) electron-withdrawing effect at C8 by a phenyl group, like in **3** and **4**, which facilitates the interaction between the carbon and N1.

The main conclusion from the crystallographic analysis is that the molecular conformation seems to be the most important factor in reactivity of the thermolabile carbonates. Nucleophilicity of pyridine is necessary but insufficient in the process of thermocyclisation, dominated by the molecules' ability to adopt a favorable conformation.

The main conclusion from the NMR analysis in solution is finding that the key element of the structure, which affects the activity of TGO, is the presence (or lack) of *exo*-amine protons. In all molecules with *exo*-amine protons, no strong NOEs were observed for an interaction between the pyridine hydrogen with distant parts of the compound. This suggests that the first torsion angle N1–C2–N2–C7 has values rather close to *anti* conformation. A quite different situation occurs in **1** in which the labile *exo*-amine proton is absent. In the solution and in the crystal, the first torsion angle N1–C2–N2–C7 in **1** is close to the *syn* conformation (this conformation is proposed as necessary for thermocyclization). The most effective seems to be the steric effect observed in **1**. The introduction of a large benzyl group in the immediate vicinity of the pyridyl ring changes orientation of the molecule in such a way that the pyridyl ring is located in close relation to the C8 atom. In addition, this compound has the advantage of not being chiral (like **3** and **4**). Weakening or strengthening the nucleophilicity of the pyridyl nitrogen through electronic effects and tautomerism play a minor role. The presence of a phenyl group with the secondary carbon atom C8 directly connected with the hydroxyl group does not affect the nucleophilic character of the pyridyl ring but impacts the kinetics of cyclization, increasing the susceptibility of the carbon atom to a nucleophilic attack. On the other hand, a large substituent at the *exo*-amine N2 position helps the molecule in acquiring a conformation with shortening of the N1···C8 distance. With this and other suggestions presented in this article, compound **1** and its derivatives are promising precursors of thermolabile protecting groups.

Experimental methods

General remarks

All reagents (analytical grade) were obtained from commercial suppliers and used without further purification. Hexane and

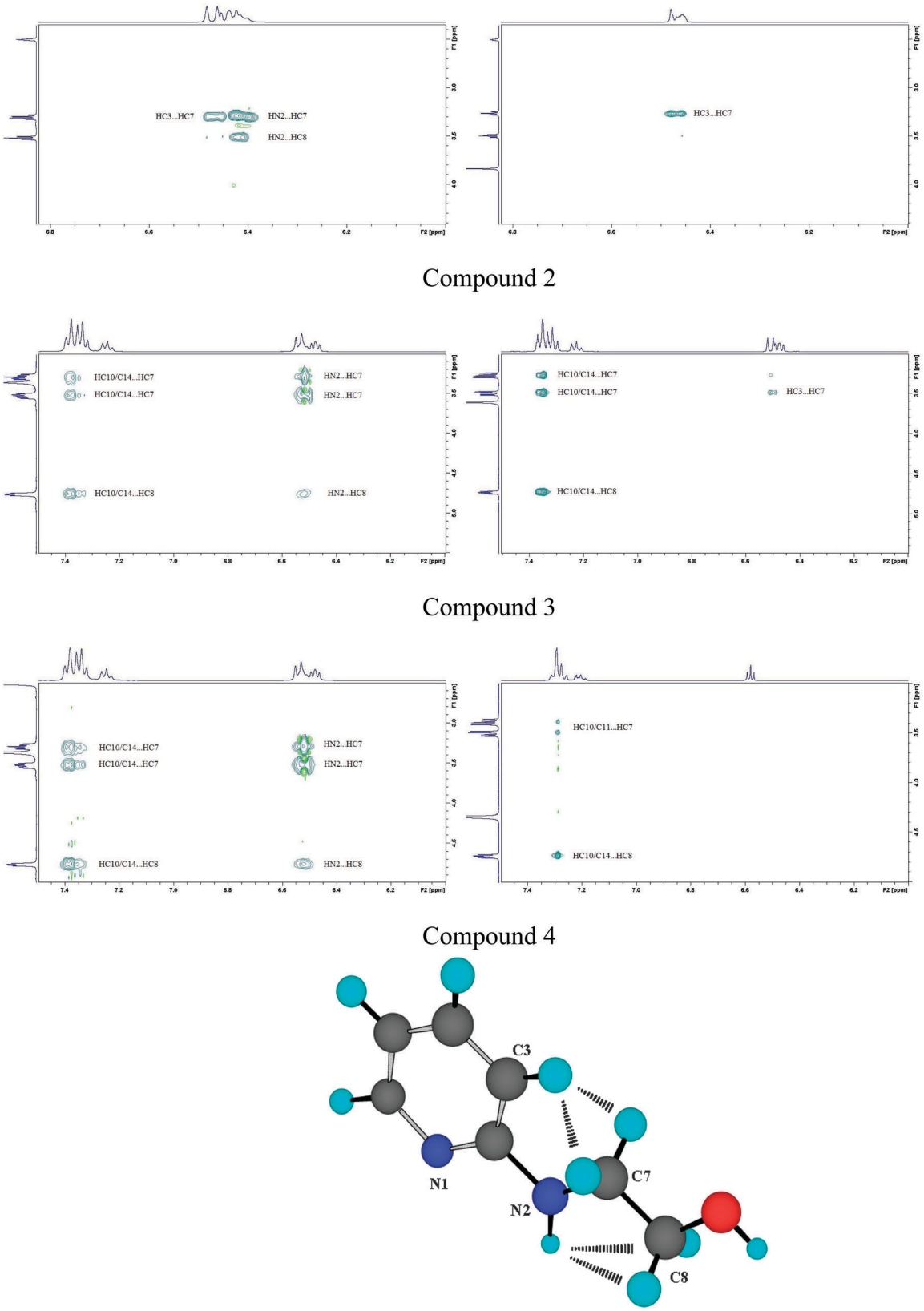

Fig. 4 The expanded NOESY contour plots for **2**, **3** and **4**. On the left—a spectrum recorded in DMSO, on the right—recorded after shaking with D_2O. At the bottom—the model of interaction in solution shown on the example of compound **2**.

dichloromethane were freshly distilled from CaH_2 and P_2O_5, respectively. All other solvents and liquid reagents were dried through storage over activated 3 Å (MeOH, MeCN) molecular sieves.

^1H, ^{13}C NMR and two dimensional spectra: the NMR spectra were recorded at 298 K on a spectrometer operating at frequencies 400.13201 MHz (^1H) and 100.62281 MHz (^{13}C).

Liquid secondary ion mass spectrum (low and high resolution) was obtained on two sector mass spectrometers of reverse B/E geometry. A CsI gun supplied the primary ion beam (12 keV, Cs+). The secondary ion beam was accelerated to 8 kV. The compound was dissolved in 3-nitrobenzyl alcohol.

General procedure for the preparation of *N*-(2-pyridylo)aminoethanol (1–4)

2-Bromopyridine (1.58 g, 10 mmol) and suitable aminoethanol (20 mmol) were heated for 48 h in an oil bath and kept at 140 °C. The reaction mixture was then allowed to cool to ambient temperature and dichloromethane (250 mL) was added. The solution was shaken with a saturated solution of sodium carbonate (200 mL). The organic layer was dried over anhydrous magnesium sulfate and evaporated to dryness. The product was purified by silica gel chromatography by means of dichloromethane/methanol (9.9/0.1). The product underwent crystallization at 0 °C from oil.

N-(2-Pyridyl)*N*-benzylaminoethanol (1)

^1H NMR (300 MHz, DMSO-d_6) δ 8.06 (dd, J = 1.38, 4.86 Hz, 1H); 7.43 (2 × dd, J = 2.01, 7.03 Hz, 1H); 7.25 (m, 5H); 6.58 (dt, J = 1.38, 8.67 Hz, 1H); 6.54 (dd, J = 4.95, 7.03 Hz, 1H); 4.79 (s, 2H), 3.59 (m, 4H).

^{13}C NMR (75 MHz, DMSO-d_6) δ 157.8, 147.4, 139.2, 137.2, 128.3, 126.5, 111.5, 105.8, 58.63, 51.42, 50.4.

HR MS (LSI)[M−H$^-$] calcd for $C_{14}H_{16}N_2O$, 229.13409; found, 229.13382.

N-(2-Pyridyl)amino-1-ethanol (2)

^1H NMR (300 MHz, DMSO-d_6) δ 7.94 (dd, J = 1.25, 5.05 Hz, 1H); 7.33 (dd, J = 1.99, 7.09 Hz, 1H); 6.48 (d, J = 8.5 Hz, 1H); 6.44 (dd, J = 7.09 Hz, 1H); 6.42 (m, 1H); 4.76 (m, 1H); 3.52 (t, J = 6.01 Hz, 2H); 3.31 (q, J = 5.82, 6.01 Hz, 2H).

^{13}C NMR (75 MHz, DMSO-d_6) δ 43.9, 60.6, 108.6, 111.8, 137.0, 147.8, 159.3.

HR MS (LSI)[M−H$^-$] calcd for $C_7H_{10}N_2O$, 139.08714; found, 139.08638.

N-(2-Pyridyl)amino-1-phenyloethanol (3)

^1H NMR (300 MHz, DMSO-d_6) δ 7.97 (dd, J = 1.16, 4.95 Hz, 1H); 7.35 (m, 5H); 7.24 (t, J = 7.23 Hz, 1H); 6.52 (m, 2H); 6.47 (t, J = 6.47 Hz, 1H); 5.68 (s, 1H); 4.76 (q, J = 4.4 Hz, 1H); 3.52 (ddd, J = 4.4, 6.5, 13.2 Hz, 1H); 3.28 (td, J = 4.93, 13.05 Hz, 1H).

^{13}C NMR (75 MHz, DMSO-d_6) δ 159.3, 147.7, 144.7, 137.1, 128.4, 127.3, 126.4, 112.05, 109.05, 72.05, 49.7.

HR MS (LSI)[M−H$^-$] calcd for $C_{13}H_{14}N_2O$, 215.11844; found, 215.11905.

N-(2-Pyrimidyl)amino-1-phenyloethanol (4)

^1H NMR (300 MHz, DMSO-d_6) δ 8.27 (d, J = 4.77 Hz, 2H); 7.3 (m, 5H); 6.96 (t, J = 4.76 Hz, 1H); 6.56 (t, J = 4.77 Hz, 1H); 5.5 (d, J = 4.06 Hz, 1H); 4.7 (q, J = 3.8, 7.6 Hz, 1H); 3.54 (ddd, J = 4.72 Hz, 1H); 3.4 (m, 1H).

^{13}C NMR (75 MHz, DMSO-d_6) δ 49.5, 71.5, 110.6, 126.5, 127.4, 128.4, 144.4, 158.4, 162.7.

HR MS (LSI)[M−H$^-$] calcd for $C_{12}H_{13}N_3O$, 216.11369; found 216.11369.

Bis[*N*-(2-pyridyl)aminoethyl]carbonate (5)

2-(2-Pyridyl)aminoethanol (578 mg, 2 mmol) and carbodiimidazole (162 mg, 1 mmol) were dissolved in dry acetonitrile (5 mL). After 1 hour 1,1,3,3-tetramethylguanidine (0.3 mL) was added, and the mixture was kept at 5 °C for 12 hours. TLC analysis showed that reaction was completed. The reaction mixture was partitioned between saturated $NaHCO_3$ (80 mL) and dichloromethane (100 mL). The organic layer was dried, concentrated under reduced pressure and purified by silica gel column chromatography with dichloromethane. The final product underwent crystallization with organic layers (dichloromethane/hexane 3 : 1).

^1H NMR (300 MHz, DMSO-d_6) δ 7.96 (dd, J = 1.85, 4.94 Hz, 1H); 7.35 (dd, J = 1.96, 7.03 Hz, 1H); 6.67 (t, J = 5.6 Hz, 1H); 6.49 (m, 1H); 6.47 (m, 1H); 4.19 (t, J = 5.7 Hz, 1H); 3.51 (q, J = 5.56 Hz, 1H).

^{13}C NMR (75 MHz, DMSO-d_6) δ 39.5, 66.8, 108.9, 112.2, 137.1, 147.9, 151.2, 155.1, 158.9.

HR MS (LSI)[M−H$^-$] calcd for $C_{15}H_{18}N_4O_3$, 303.14572; found, 303.14464.

X-Ray diffraction data were obtained up to the resolution of 0.75–0.76 Å on the X13 EMBL beamline at the DESY synchrotron, Hamburg, Germany. During data collection the crystals remained in the cryo-stream of cold nitrogen gas at 100 K. The diffraction images were recorded on a 165 mm detector. The diffraction intensities were integrated and scaled using the program.[15] The X-ray data are summarized in Table 2. The crystal structures were solved by direct methods and refined using the program SHELIX.[16]

CCDC 827067 for **1**, CCDC 827068 for **2**, CCDC 827069 for **3**, CCDC 827070 for **4**, and CCDC 827071 for **5.**

Acknowledgements

This work was supported by the Polish State Committee for Scientific Research grant No 3 T09A 116 27 and by the European Community Research Infrastructure Action under the F6P "Structuring the European Research Area Programme" (contract number RII3/CT/2004/5060008).

References

1 A. Grajkowski, J. Cieslak, M. K. Chmielewski, V. Marchan, L. R. Phillips, A. Wilk and S. L. Beaucage, *Ann. N. Y. Acad. Sci.*, 2003, **1002**, 1–22.
2 A. Ohkubo, R. Kasuya, K. Miyata, H. Tsunoda, K. Seio and M. Sekine, *Org. Biomol. Chem.*, 2009, **7**, 687–694.
3 A. Grajkowski, A. Wilk, M. K. Chmielewski, L. R. Phillips and S. L. Beaucage, *Org. Lett.*, 2001, **3**, 1287–1290.

4 (*a*) A. Wilk, M. K. Chmielewski, A. Grajkowski, L. R. Phillips and S. L. Beaucage, *Tetrahedron Lett*., 2001, **42**, 5635–5639; (*b*) A. Wilk, M. K Chmielewski, A. Grajkowski, L. R. Phillips and S. L. Beaucage, in *Current Protocols in Nucleic Acid Chemistry*, ed. S. L. Beaucage, D. E. Bergstrom, G. D. Glick and R. A. Jones, John Wiley & Sons, New York, 2002, pp. 3.9.1–3.9.15.
5 A. Wilk, M. K. Chmielewski, A. Grajkowski, L. R. Phillips and S. L. Beaucage, *J. Org. Chem*., 2002, **67**, 6430–6438.
6 J. Cieslak and S. L. Beaucage, *J. Org. Chem*., 2003, **68**, 10123–10129.
7 A. P. Guzaev and M. Manoharan, *J. Am. Chem. Soc*., 2001, **123**, 783–793.
8 M. K. Chmielewski, *Org. Lett*., 2009, **11**, 3742–3745.
9 (*a*) H. Giegrich, S. Eisele-Buhler, C. Hermann, E. Kvasyuk, R. Charubala and W. Pfleiderer, *Nucleosides Nucleotides*, 1998, **17**, 1987–1996; (*b*) S. Buhler, H. Giegrich and W. Pfleiderer, *Nucleosides Nucleotides*, 1999, **18**, 1281–1283.
10 S. L. Beaucage and M. K. Chmielewski, *PCT Int. Appl*.,, *WO*2004101582, 2004.
11 M. K. Chmielewski, V. Marchan, J. Cieslak, A. Grajkowski, V. Livengood, U. Munch, A. Wilk and S. L. Beaucage, *J. Org. Chem*., 2003, **68**, 10003–10012.
12 N. Weiner and I. A. Kaye, *J. Org. Chem*., 1949, **14**, 868–872.
13 The analysis of thermolability of carbonates from compound **4** was placed on ESI.† The total time of deprotection that the carbonates obtained from precursor **4** was determined as 30 min (90 °C in acetonitrile/buffer pH = 7).
14 F. H. Allen, O. Kennard, D. G. Watson, L. Brammer, A. G. Orpen and R. Taylor, *J. Chem. Soc., Perkin Trans. 2*, 1987, **12**, 1–19.
15 Z. Otwinowski and W. Minor, *Methods Enzymol*., 1997, **276**, 307–326.
16 G. M. Sheldrick, *Acta Crystallogr., Sect. A: Found. Crystallogr*., 2008, **64**, 112–122.

